J Solid State Electrochem (2000) 4: 210–215

ORIGINAL PAPER

Roberto Herrera Sánchez · Leopoldo Treviño
Antonio F. Fuentes · Azael Martínez-de la Cruz
Leticia M. Torres-Martínez

Electrochemical lithium insertion in two polymorphs of a reduced molybdenum oxide (γ and γ'- Mo_4O_{11})

Received: 20 April 1999 / Accepted: 20 June 1999

Abstract A study of the electrochemical lithium insertion in two polymorphs of a reduced molybdenum oxide, Mo_4O_{11}, is presented in this work. When used as active materials in cells discharged down to 1 V vs. Li^+/Li, both forms, the orthorhombic γ-Mo_4O_{11} and the monoclinic γ'-Mo_4O_{11}, incorporated a similar number of lithium atoms per metal atom (Li/Mo = 2.12 and 2.25, respectively). Step potential electrochemical spectroscopy experiments proved that the insertion reaction proceeds in both cases through different mechanisms. In situ X-ray diffraction studies showed an almost complete loss of crystallinity of both compounds after the first discharge, leading to amorphous materials with different electrochemical behaviour on cycling. When discharged to low potentials (0.5 V vs. Li^+/Li), the γ'-Mo_4O_{11} polymorph showed very good cycling behaviour for at least five lithium atoms per formula unit, corresponding to a specific capacity of 230 Ah/kg after seven complete charge-discharge cycles.

Key words Lithium insertion · Reduced molybdenum oxide · Step potential electrochemical spectroscopy · X-ray diffraction

Introduction

The potential application of different molybdenum phases in energy storage systems has been studied since the early stages of research in this field of solid state ionics, showing promising results [1–3]. In this work we have studied the electrochemical insertion of lithium into two forms of a reduced molybdenum oxide, Mo_4O_{11}. The structural framework of the two polymorphs of Mo_4O_{11} contains two different coordination polyhedra: regular MoO_4 tetrahedra and distorted MoO_6 octahedra. The octahedra are linked together by corner sharing, forming ReO_3-type slabs mutually connected by MoO_4 tetrahedra which share corners with the octahedra of the two neighbouring slabs: three with two octahedra in one slab and the remaining corner with an octahedron in the next slab. The basic difference between the orthorhombic and monoclinic forms lies on the relative orientation of neighbouring slabs, giving place to different 3D tunnels where additional ions can be incorporated [4]. A total of 10 four-sided and 4 five-sided tunnels are found in a unit cell of the orthorhombic form, while 12 four-sided and 2 six-sided tunnels can be found on the monoclinic one (Fig. 1).

The Mo_4O_{11} behaviour versus the electrochemical lithium insertion has been studied by Christian et al. [5], who pointed out that down to 1.5 V and after 20 charge/discharge cycles it shows a reversible capacity of >0.75 Li/Mo. By treating Mo_4O_{11} with an excess of *n*-butyllithium, they also estimated 1.62 Li/Mo as the limiting value of lithium incorporation in this oxide and calculated a theoretical energy density of the order of 400–500 Wh/kg. They also suggested that cycling this material below 1.4 V would lead to a lower cell capacity because of irreversible changes on the structure of the pristine material. Nothing was said about which form of Mo_4O_{11} was used in this study. In the light of some results published by different authors about the good cycling behaviour of some crystalline and amorphous 3D framework structures when discharged to very low voltages [3, 6–8], we decided to further investigate lithium insertion in this molybdenum oxide.

R.H. Sánchez · L. Treviño · A.F. Fuentes (✉)
A. Martínez-de la Cruz · L.M. Torres-Martínez
Facultad de Ciencias Químicas,
División de Estudios Superiores,
Universidad Autónoma de Nuevo León,
Apartado Postal 1625, Monterrey,
Nuevo León, México
e-mail: afernand@ccr.dsi.uanl.mx
Tel.: +52-83-741188/728065 ext. 113/115
Fax: +52-83-744937/740709

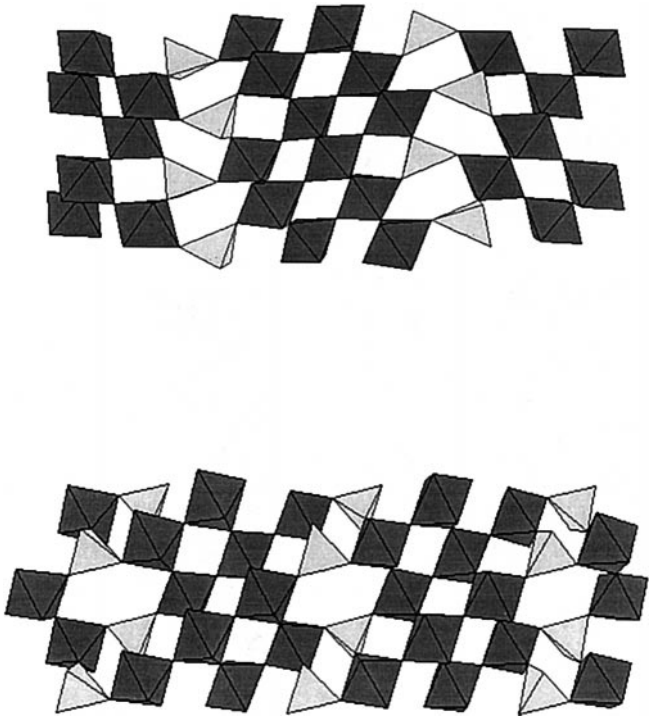

Fig. 1 Idealized structures of γ (*top*) and γ'-Mo_4O_{11} (*bottom*) showing the different coordination polyhedra, MoO_4 and MoO_6, and tunnels present in these compounds

Experimental

Preparation and characterisation of γ-Mo_4O_{11} and γ'-Mo_4O_{11}

The two polymorphs γ-Mo_4O_{11} and γ'-Mo_4O_{11}, were prepared by a solid state reaction. The starting materials, MoO_3 (Aldrich 99.5%) and MoO_2 (Aldrich 99.0%), were weighed in the appropriate stoichiometric ratio (3:1 MoO_3:MoO_2) and thoroughly mixed by grinding in an agate mortar under Analar grade acetone. The mixed powders were placed in quartz ampoules which, after being evacuated and sealed, were taken to an electrical furnace. The orthorhombic γ-Mo_4O_{11} was obtained as described in the literature, after firing the reaction mixture for 8 days at 660 °C, while the monoclinic γ'-Mo_4O_{11} was obtained by heating for 17 days at 550 °C [9]. Phase identification was carried out by X-ray powder diffraction in a Siemens D-5000 diffractometer using Cu-Kα radiation ($\lambda = 1.5418$ Å). A typical diffraction experiment for determining cell parameters was run with a step size of 0.12°/min using Al_2O_3 as internal standard.

Electrochemical lithium insertion

Electrochemical experiments were carried out in a multichannel potentiostatic-galvanostatic system MacPile II [10], using Swagelok-type test cells [11] with lithium metal acting simultaneously as both negative and reference electrodes. Positive electrodes were prepared by mixing and pressing a mixture of the phase being tested with carbon black and a binder, (0.5% ethylene-propylene-diene terpolymer, in cyclohexane) in a 89:10:1 ratio (wt%). The electrolyte used was an 1 mol dm^{-3} solution of $LiClO_4$ in a previously dried 50:50 mixture of ethylene carbonate and diethoxyethane [12]. Cell assemblage was carried out in a MBraun glove box under an argon atmosphere and with a continuous purge of water vapour and oxygen, ensuring a concentration in both cases smaller than 1.5 ppm.

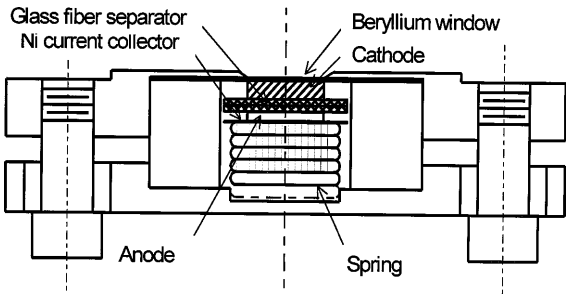

Fig. 2 Schematic representation of the electrochemical cell built for in situ X-ray diffraction experiments

Electrochemical experiments were carried out either in a current-controlled or in a potential-controlled mode. Potentiodynamic titrations were carried out by a stepwise technique also known as "step potential electrochemical spectroscopy" (SPECS) [13]. Typical experimental conditions were set at ± 10 mV/h potential steps with a charge recording resolution of 5 μmAh and keeping the temperature controlled (± 2 °C).

Electrochemical cell for in situ X-ray diffraction studies

In order to study the influence of the insertion reaction on the structure of the parent oxides, an electrochemical cell was built to fit in our Siemens D-5000 diffractometer. Such a cell consists of two metal parts built with stainless steel ASTM 1025: (1) a cell top which holds a beryllium window where cathode materials (prepared as described above), were deposited by spreading them as a slurry mixed with acetone or directly as a pellet and (2) a cell base. Lithium metal was placed on the cell base pasted on a nickel disk acting as a current collector for the negative electrode. Two layers of S&S no. 25 glass fibre separator soaked on the electrolyte were placed between the electrodes. The cell also features a spring which ensures physical contact between the different parts and allows a tight seal. All these elements were placed inside a Teflon casing which prevents the cell short-circuiting. Figure 2 shows a schematic representation of this cell. When mounted on the diffractometer, the cell was electrically isolated to prevent self-discharge. Electrochemical experiments for in situ X-ray studies were carried out by discharging this cell in a current-controlled mode to predetermined "x" values in $Li_xMo_4O_{11}$. Once each chosen composition was reached, the circuit was open so that the system could reach equilibrium conditions and allow X-ray diffraction patterns to be collected with approximately 1 h exposure time to X-rays.

Results and discussion

Figure 3 shows the evolution of cell voltage with composition (x in $Li_xMo_4O_{11}$) for both polymorphs obtained from the SPECS experiments. These results show that when discharged down to 1 V using -10 mV/h potential steps, both γ-Mo_4O_{11} (solid circles/solid line) and γ'-Mo_4O_{11} (open squares/dashed line) incorporated a similar number of lithium atoms per formula unit, 8.5 and 9 respectively (Li/Mo = 2.12 and 2.25), although apparently not through the same mechanisms. The main features of the graph obtained for the monoclinic γ'-Mo_4O_{11} are three very well-defined plateaux labelled in Fig. 3 as I′, II′ and III′, with approximately constant E values around 2.40, 2.20 and 1.90 V vs. Li^+/Li,

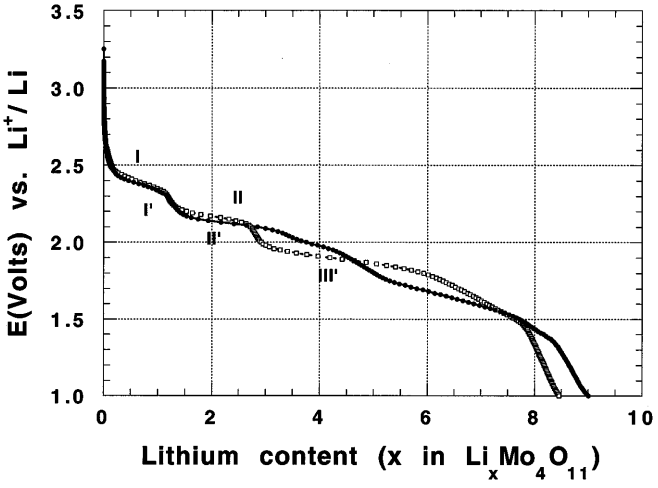

Fig. 3 Evolution of cell voltage with composition (x in $Li_xMo_4O_{11}$) obtained when discharging (−10 mV/h) two electrochemical cells using γ-(*solid circles*/*solid line*) and γ'-Mo_4O_{11} (*open squares*/*dashed line*) as active materials of the positive electrodes

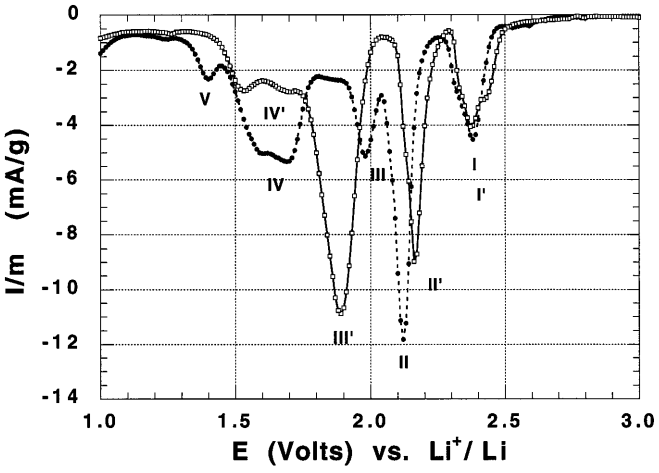

Fig. 4 I/m vs. E representations of the insertion-induced reduction process of γ (*solid circles*/*dashed line*) and γ'-Mo_4O_{11} (*open squares*/*solid line*) obtained from SPECS experiments run at −10 mV/h

respectively. These plateaux might correspond to continuous transformations or to two-phase systems and separate several regions of continuous variation of E with composition including one, below 1.80 V ($x > 6$), with various slope changes. Slightly different electrochemical behaviour was observed in the cells using the orthorhombic γ-Mo_4O_{11} as the active material of the positive electrode. Figure 3 shows that, in this case, only two very well-defined plateaux, labelled as I and II, can be seen at approximately 2.40 and 2.10 V vs. Li^+/Li. These plateaux can be related to I′ and II′ observed in γ'-Mo_4O_{11}, although in γ-Mo_4O_{11} the second one seems to cover a larger composition range. After this second plateau, a succession of various slope changes can be observed, although in this representation it is not possible to identify the presence of a plateau similar to III′.

Differences in the electrochemical characteristics of lithium insertion in both polymorphs of Mo_4O_{11} are more evident in Fig. 4. This graph shows a representation of I/m (mA/g) vs. E (V) for both polymorphs obtained from the SPECS experiments run at −10 mV/h potential steps. Results obtained for the orthorhombic γ-Mo_4O_{11} (solid dots/dashed line) show the existence of at least five very well-defined reduction steps on lithium insertion, which are labelled as I, II, III, IV and V. On the other hand, the curve obtained with the monoclinic γ'-Mo_4O_{11} (open squares/solid line) shows four very well-defined reduction steps, labelled as I′, II′, III′ and IV′. While the first reduction steps, I and I′, are observed almost at the same voltage in both polymorphs, differences are gradually building up as the insertion-induced reduction proceeds to lower voltages. The main difference is found on the third reduction step, which in the monoclinic γ'-Mo_4O_{11} seems to cover a wider voltage interval when compared with its homologue in the orthorhombic γ-Mo_4O_{11}. Additionally, no reduction step equivalent to V (below 1.5 V vs. Li^+/Li) is found in the monoclinic γ'-Mo_4O_{11}.

In order to clarify the nature of such reduction steps, insertion reaction kinetics were examined more in detail. For reason of clarity, each of the two polymorphs will be studied separately and later compared.

γ-Mo_4O_{11}

Figure 5 shows a chronoamperogram obtained during the first discharge down to 1.2 V (−10 mV/h) of a cell with the configuration Li//γg-Mo_4O_{11}. The time dependence of the current (I vs. time plots) shows, for the first three steps, a profile obviously not governed by a simple diffusion process which would give a monotonic tendency towards $I = 0$ but is typical of a two-phase system. Step I seems to be formed by more than one process while step II shows a current relaxation versus time profile at each voltage step, typical of a two-phase system with a growing contact area between phases. The

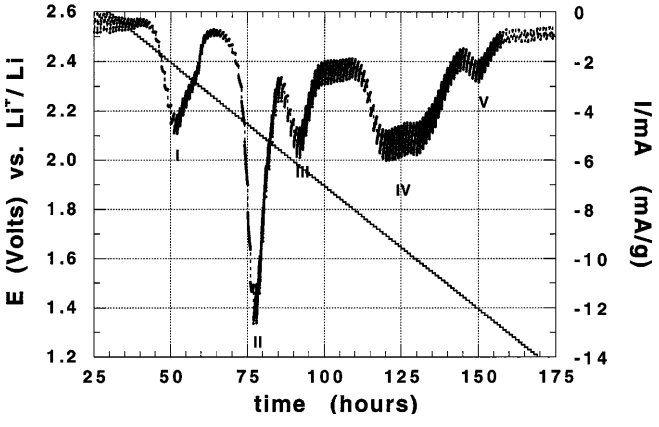

Fig. 5 Chronoamperogram obtained during the first discharge (−10 mV/h) of a cell with the configuration Li//γ-Mo_4O_{11}, showing the time dependence of the cell current

open-circuit two-phase equilibrium potential in these systems can be given as the intercept at the slope extrapolations to zero current, i.e. 2.47, 2.20 and 2.08 V vs. Li^+/Li, respectively. The *I* vs. time plot indicates also that in step IV the system is crossing at least another two multiphase systems, while step V seems to be also a two-phase system.

In situ X-ray diffraction experiments (Fig. 6), showed a gradual and irreversible loss of crystallinity as the insertion reaction proceeds, leading to a material with a diffraction pattern almost featureless, typical of an amorphous compound.

γ'-Mo_4O_{11}

Figure 7 shows the current relaxation versus time plot for the monoclinic polymorph obtained from SPECS experiments when discharging a cell with the configuration $Li//\gamma'$-Mo_4O_{11} using −10 mV/h potential steps. In this case the first three reduction steps show a similar profile, typical of two-phase systems with open-circuit equilibrium potentials between phases of 2.50, 2.13 and 2.02 V vs. Li^+/Li. These three steps can be related to those observed in the insertion-induced reduction of γ-Mo_4O_{11} and labelled as I, II and III, although III′ covers a larger potential region than its homologue. The nature of the step labelled as IV′ could not be confirmed with the data obtained in this experiment, although it seems to be formed by various processes. In this case, in situ x-ray diffraction experiments (Fig. 8), also showed a complete loss of crystallinity as the insertion reaction proceeds, a characteristic that remains after completing a charge-discharge cycle.

In order to determine whether lithium insertion/de-insertion in these polymorphs was a reversible process,

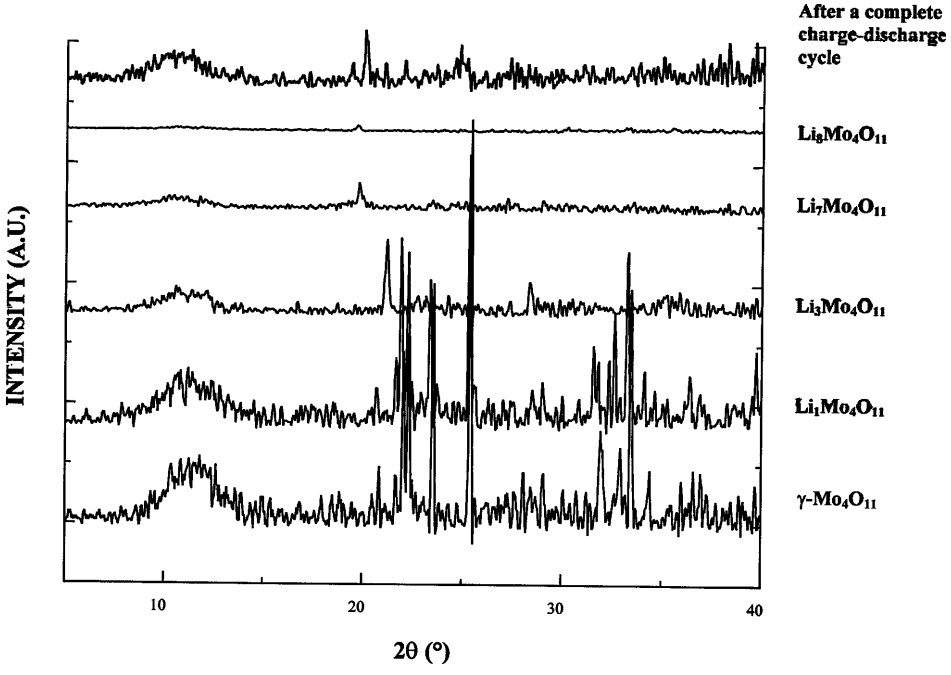

Fig. 6 Evolution of the γ-Mo_4O_{11} X-ray diffraction pattern as the insertion reaction proceeds, showing a gradual loss of crystallinity as the number of lithium atoms increases

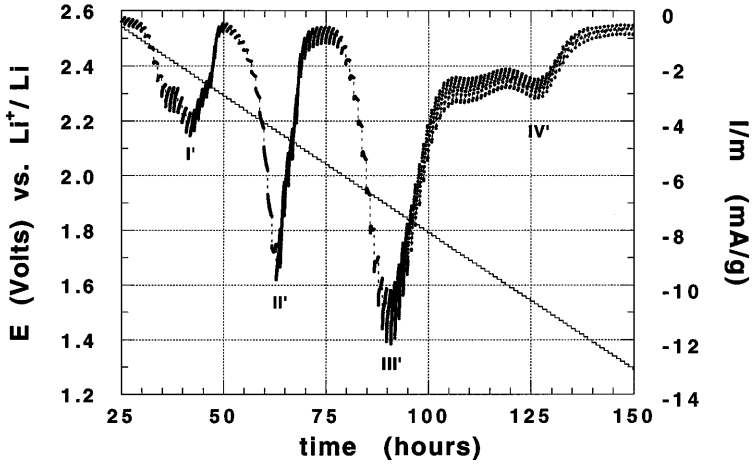

Fig. 7 Chronoamperogram obtained during the first discharge (−10 mV/h) of a cell with the configuration $Li//\gamma'$-Mo_4O_{11}, showing the time dependence of the cell current

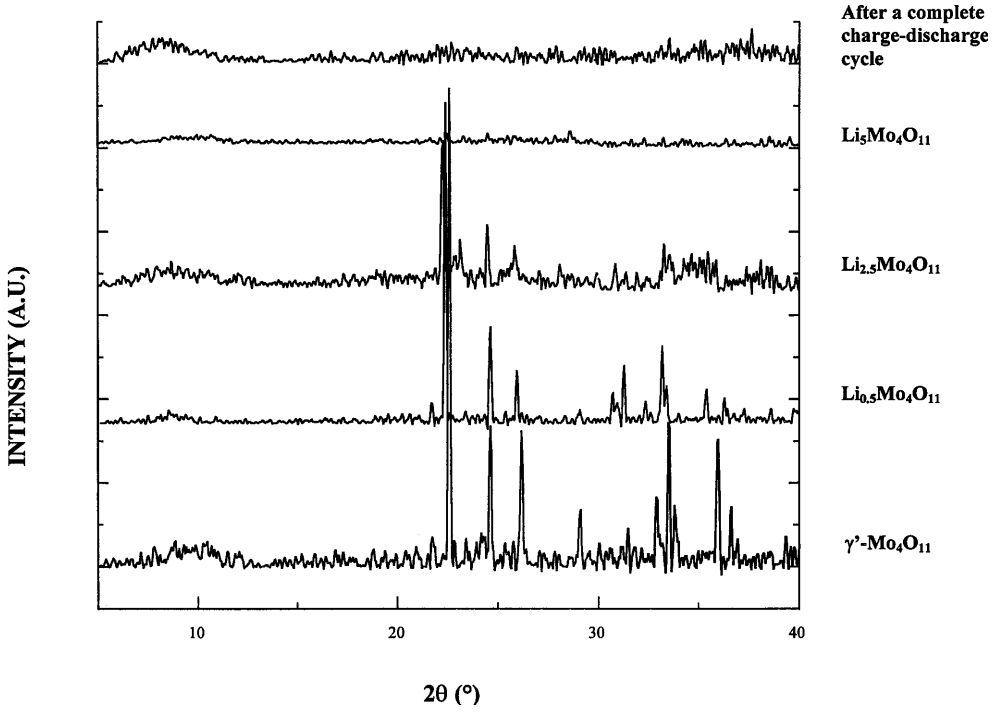

Fig. 8 Evolution of the γ-Mo_4O_{11} X-ray diffraction pattern as the insertion reaction proceeds, showing a gradual loss of crystallinity as the number of lithium atoms increases

several charge-discharge cycles were completed between different voltage limits in two cells similar to the ones mentioned above. The experiments run down to 1 V (not shown) showed that lithium insertion/deinsertion in γ- and γ'-Mo_4O_{11} is not a reversible process, with a large number of the atoms initially inserted remaining in the structures after completing a charge-discharge cycle and showing also a gradual capacity loss on cycling. Therefore, both compounds were irreversibly transformed leading to amorphous mixtures, which showed poor performance on cycling. Surprisingly, when running experiments down to 0.5 V, the monoclinic γ'-Mo_4O_{11} showed different electrochemical behaviour from that previously found. As shown in Fig. 9, the material formed after the initial discharge showed very good cycling performance for at least five lithium atoms (Li/Mo = 1.25), corresponding to a specific capacity of 230 Ah/kg after seven complete charge-discharge cycles. These results were obtained from galvanostatic experiments run at a cycling rate greater than C/42 after the first discharge (C/42 corresponds to a charge or a discharge within 42 h). However, the cycling characteristics of lithium insertion in the orthorhombic γ-Mo_4O_{11} did not improve in these new limits, showing a large capacity fade after the first complete cycle with additional losses on cycling (Fig. 10). These differences in the electro-

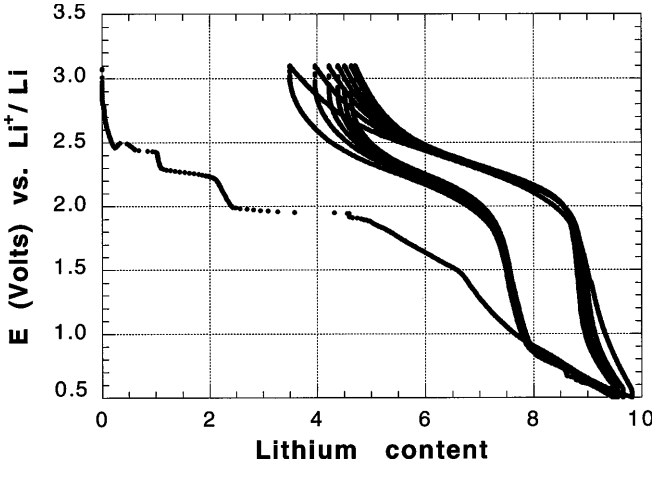

Fig. 9 Evolution of cell voltage with composition (seven cycles) for a cell with the configuration Li//γ'-Mo_4O_{11}, showing very good cycling behaviour for at least five lithium atoms

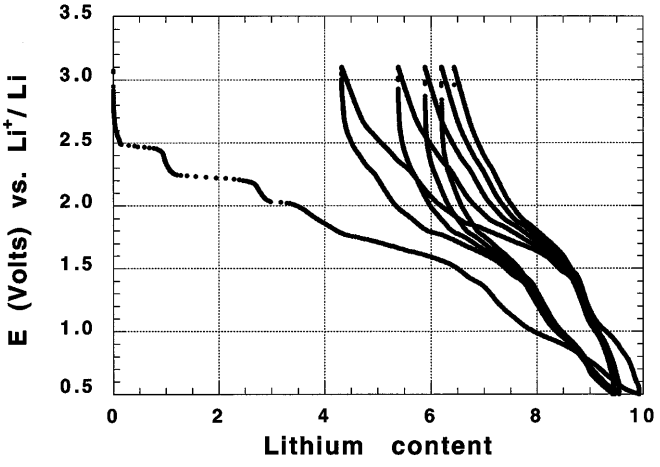

Fig. 10 Evolution of cell voltage with composition (five cycles) for a cell with the configuration Li//γ-Mo_4O_{11}

chemical behaviour of both compounds suggest that the material formed during the insertion-induced reduction of γ-Mo_4O_{11} is different from the one obtained after reducing γ'-Mo_4O_{11}.

Conclusions

A study of lithium insertion in the two polymorphs of a reduced molybdenum oxide, Mo_4O_{11}, was carried out in this work. SPECS experiments run down to 1 V vs. Li^+/Li showed that the insertion-induced reduction of γ- and γ'-Mo_4O_{11} goes through different mechanisms and leads to different materials with at least five reduction steps in the first case and four in the second. A study of insertion reaction kinetics in these steps suggested the presence of two-phase systems. In situ X-ray diffraction studies showed a gradual and irreversible loss of crystallinity as the lithium insertion proceeds, leading in both cases to amorphous materials with different electrochemical behaviour to that of the pristine phases. Cells using the monoclinic γ'-Mo_4O_{11} as active material for the positive electrode showed a very good cycling performance after the first discharge down to 0.5 V vs. Li^+/Li, incorporating reversibly five lithium atoms which correspond to a specific capacity of 230 Ah/kg after seven complete charge-discharge cycles.

Acknowledgements Financial support from CONACYT (projects 3862P-A9607 and 3824P-A9607) and UANL (grant PAICYT CA060-98) is gratefully acknowledged.

References

1. Dampier FW (1974) J Electrochem Soc 121: 656
2. Besenhard JO, Schöllhorn R (1976/77) J Power Sources 1: 267
3. Leroux F, Goward GR, Power WP, Nazar LF (1998) Electrochem Solid State Lett 1: 255
4. Kihlborg L (1963) Ark Kemi 21: 471
5. Christian PA, Carides JN, DiSalvo FJ, Waszczak JV (1980) J Electrochem Soc 127: 2315
6. Sigala C, Guyomard D, Piffard Y, Tournoux M (1995) CR Acad Sci Paris Ser IIb 320: 523
7. Denis S, Baudrin E, Touboul M, Tarascon J-M (1997) J Electrochem Soc 144: 4099
8. Idota Y (1993) Eur Pat 0 567 149 A1
9. Magnéli A (1948) Acta Chem Scand 2: 861
10. Mouget C, Chabre Y: Multichannel potentiostatic and galvanostatic system MacPile. Bio-Logic, Claix, France
11. Tarascon J-M (1985) J Electrochem Soc 132: 2089
12. Guyomard D, Tarascon J-M (1992) J Electrochem Soc 139: 97
13. Chabre Y (1991) J Electrochem Soc 138: 329